Three Dimensional Centerline Reconstruction using Multiplane Discrete Dynamic Curves

Joeri CHRISTIAENS   Rik VAN DE WALLE   Ignace LEMAHIEU

ELIS-MEDISIP
Ghent University
Sint-Pietersnieuwstraat 41, 9000 Ghent
BELGIUM

Abstract: - In cardiac catheterization labs, x-ray angiography is used to visualize abnormal narrowings of the coronary arteries, i.e., stenoses. An often used technique to treat stenoses is stent implantation. This technique can only be performed successfully if the length of the stenotic lesion and the radius of the non-stenotic part of the narrowed vessel segment are known precisely. In clinical practice, the determination of these quantities is done directly based on angiographic images of the coronary arteries or based on a three dimensional reconstruction of the coronary arteries build up using (two) angiographic images. In this paper, a method is presented to build up a three dimensional reconstruction of the centerline of the coronary arteries using more than two angiographic images. This is a preparatory step to build a complete reconstruction of the arteries based on more than two images. The presented method is based on discrete dynamic curves. The validation is done using computer-generated phantom images.

Key-Words: - Image Processing, X-ray Angiography, Coronary Arteries, Discrete Dynamic Curves, 3-D Reconstruction

1   Introduction

In cardiac catheterization labs, coronary arteries are visualized by means of angiographic images, i.e., x-ray images of the heart region, recorded from different viewing directions after the injection of an x-ray absorbing contrast agent into the coronary arteries (See Figure 1).

Abnormal narrowings of the coronary arteries, i.e., stenoses, can be treated in a minimally invasive way by stent implantation. Doing this, the length of the stenotic lesion and the radius of the non-stenotic part of the narrowed vessel segment has to be known precisely. After all, using a stent that is too short or too small is not effective, and using a stent that is too long or too big may unnecessary damage the arteries.

Determination of quantitative parameters of a stenotic lesion directly based on angiographic images may be influenced by the viewing direction from which the arteries are visualized [1]. To deal with this viewpoint dependency, multiple computer systems have been developed that combine the information of two angiographic images and build up a three dimensional reconstruction of the coronary arteries [2]-[9]. Some systems combine the information of more than two images [10], but as far as known, these systems are not ready to be used in clinical practice yet.

In this paper, a method is presented to build up a three dimensional reconstruction of the centerline of the coronary arteries based on more than two angiographic images using discrete dynamic curves. A three dimensional centerline reconstruction is a first step towards a three dimensional reconstruction of the complete vessel structures [5].

The presented method is an extension of the work of Cañero et al. described in [11]. They use two images to reconstruct the centerline of a vessel by means of deformable curves.

Using more than two images minimizes the chance that multiple centerline configurations can be reconstructed based on the same images (described in [11]). Furthermore, it results theoretically in a better three dimensional reconstruction of
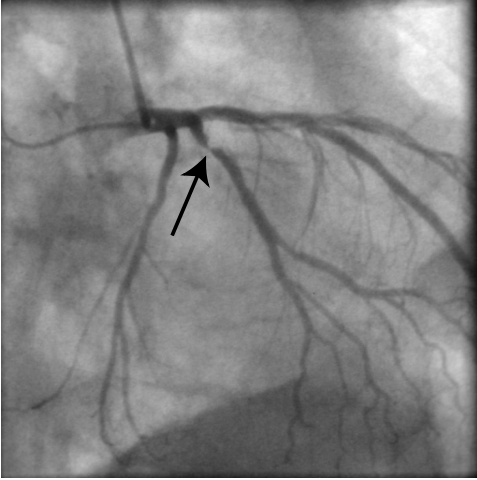
Figure 1: Angiographic image of the coronary arteries. Notice the stenosis indicated by the arrow.

Figure 2: Schematic representation of the reconstruction of a single point using two images (under ideal circumstances).

the complete vessel structures.

Starting from the terminology used in [11], i.e., *biplane snakes* for deformable curves constructed using biplane images, we will use *multiplane dynamic curves* to indicate dynamic curves constructed using more than two images.

The remaining of this paper is organized as follows: the reconstruction method is presented in Section 2, some results are given in Section 3, and a conclusion if formulated in Section 4.

2 Method

2.1 Single point reconstruction using two images

Theoretically, the three dimensional reconstruction of a single point P is the intersection of the projective lines S_1P_1 and S_2P_2 connecting the projections P_1 and P_2 of the point P with their corresponding x-ray sources S_1 and S_2, respectively (See Figure 2) [11, 12].

However, in practice, the projective lines fail to intersect due to the limited accuracy of the projection geometry, geometric image distortions and indication errors. Dumay et al. proposed to use the point P' with the minimal square distance to both projective lines as reconstructed point (See Figure 3) [12]. Today, this approximation is frequently used.
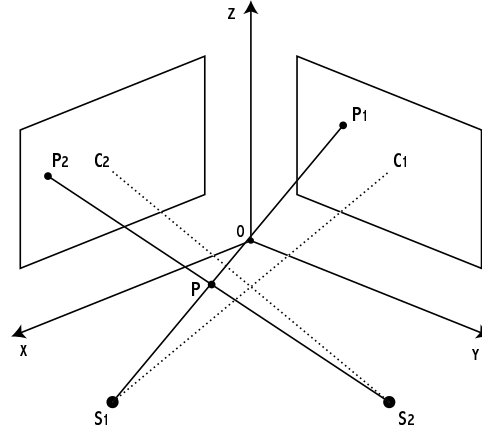
2.2 Single point reconstruction using more than two images

A schematic representation of the reconstruction of a single point using three images is shown in Figure 4.

Again, the projective lines S_1P_1, S_2P_2 and S_3P_3 fail to intersect in one particular point. As reconstructed point one can use:

- The point with the minimal square distance to all projective lines.

or

- The center of mass of the points with minimal square distance to each set of two projective lines.

Because the center of mass P'' of the points with minimal square distance to each set of two projective lines (P'_a, P'_b and P'_c in Figure 4) can easily be computed, we use this point as reconstructed point.

2.3 Discrete curve reconstruction using more than two images

Let us consider N images, a discrete target curve T_v (defined by the vertices t_1, t_2, ...), and a discrete dynamic curve Q_u (defined by the vertices q_1, q_2, ...) used to reconstruct T_v. Let $(t_v)_i$ and $(q_u)_i$ be the projections of t_v and q_u in the image plane i, respectively, with $i = 1 \ldots N$ (See Figure 5).
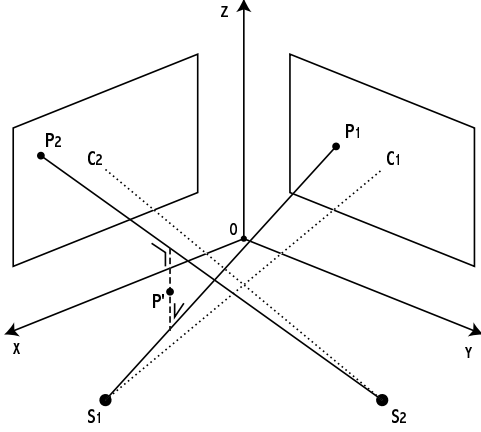
Figure 3: Schematic representation of the reconstruction of a single point using two images (under real circumstances).

Figure 4: Schematic representation of the reconstruction of a single point using three images (under real circumstances).

The curve Q_u we are looking for minimizes the error:

$$\varepsilon(Q_u) = \sum_{i=1}^{N} \sum_{j} \min_{v} \left(\| (q_j)_i - (t_v)_i \| \right) \qquad (1)$$

The initial discrete dynamic curve Q_u is obtained by connecting at least two initial vertices of which the projections are indicated in the images. The reconstruction of the initial vertices is done by means of the method described in Section 2.2. Using more than two initial vertices speeds up the curve reconstruction and is in some cases even required to find an acceptable solution.

The modification of Q_u is done by means of repeatedly resampling and deforming the dynamic curve Q_u.

2.3.1 Resampling

The method used to resample the discrete curve Q_u is a three dimensional extension of the work of Lobregt et al., presented in [13]. The desired distance between two vertices of the discrete dynamic curve is given by the parameter L_{des}. This parameter is responsible for the resolution of the curve. A big value results in a smooth curve, a smaller value allows more detail. From L_{des}, two other parameters L_{min} and L_{max} are derived, repre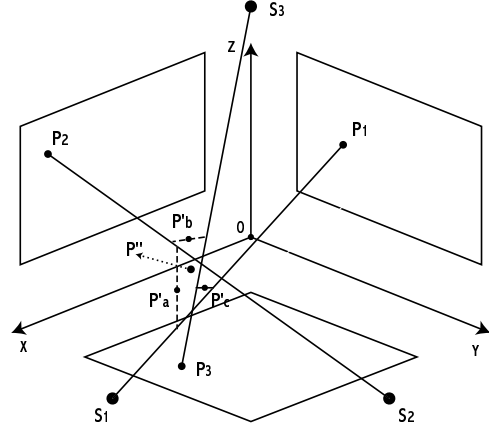senting the minimum and maximum distance which is allowed between neighboring vertices. When, during the modifications of the curve, the distance between two vertices becomes shorter than L_{min}, the two vertices are replaced by a single vertex exactly in between the two replaced vertices. When a segment becomes longer than L_{max}, an additional vertex is inserted exactly in between the two vertices. To avoid oscillations, L_{max} has to be more than two times L_{min}. We use:

$$\begin{cases} L_{min} = \frac{1}{2} L_{des} \\ L_{max} = \frac{3}{2} L_{des} \end{cases} \qquad (2)$$

2.3.2 Deforming

The curve Q_u deforms to minimize its energy:

$$E_{total}(Q_u) = E_{int}(Q_u) + E_{ext}(Q_u). \qquad (3)$$

Minimizing the internal energy E_{int} means preserving the smoothness of the curve and the equal distance between the vertices. The internal energy of a vertex q_u is:

$$\begin{aligned} E_{int}(Q_u) &= \sum_{u} \left(E_{int}(q_u) \right) \\ &\sim \sum_{u} \left(\| \overrightarrow{q_u q_{u+1}} - \overrightarrow{q_{u-1} q_u} \| \right), \quad (4) \end{aligned}$$

with q_{u-1} and q_{u+1} the vertices just before and just after q_u, respectively. The internal force used to

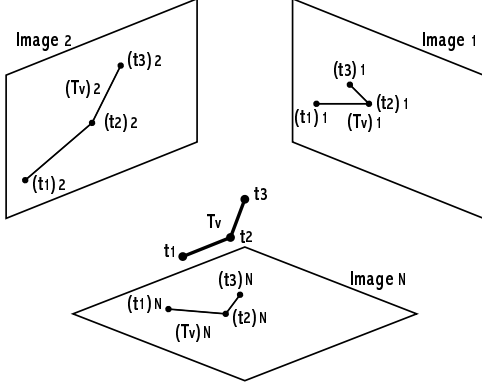Figure 5: Schematic representation of the reconstruction of a discrete curve using more than two images.

Figure 6: (left) Phantom image. (right) Surface plot of the left image representing the energy valley corresponding to the image.

minimize the internal energy of vertex q_u is:

$$\overrightarrow{F_{int}(q_u)} = \frac{\overrightarrow{q_u q_{u+1}} - \overrightarrow{q_{u-1}q_u}}{c_i}, \qquad (5)$$

with $c_i \geq 2$ to avoid oscillations.

Minimizing the external energy E_{ext} means deforming the curve so that its projections coincide with the vessels. The external energy of a vertex q_u is:

$$
\begin{aligned}
E_{ext}(Q_u) &= \sum_u (E_{ext}(q_u)) \\
&\sim \sum_u \left(\sum_{i=1}^{N} PV((q_u)_i, i) \right), \qquad (6)
\end{aligned}
$$

where $PV(x, i)$ stands for the pixel value of the pixel x in the energy image i. The determination of an energy image corresponding to an angiographic image is beyond the scope of this paper. In the easiest case, the energy image equals the original image. After all, the vessels are represented by dark pixels (low pixel values $\rightarrow$ low energy), and the background consists of lighter pixels (higher pixel values $\rightarrow$ higher energy) (See Figure 1 and 6).

The external force corresponding to vertex q_u and image plane i is:

$$\overrightarrow{F_{ext,i}((q_u)_i)} = F_{ext,i}((q_u)_i)\ \overrightarrow{b_{u,i}}, \qquad (7)$$
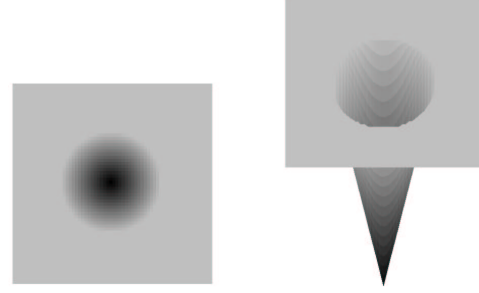
with

$$F_{ext,i}((q_u)_i) = -c_e\ \overrightarrow{\nabla PV((q_u)_i, i)} \cdot \overrightarrow{b_{u,i}}, \qquad (8)$$

and

$$\overrightarrow{b_{u,i}} = \begin{bmatrix} 0 & 1 \\ -1 & 0 \end{bmatrix} \frac{\overrightarrow{(q_{u-1})_i (q_{u+1})_i}}{\|\overrightarrow{(q_{u-1})_i (q_{u+1})_i}\|}, \qquad (9)$$

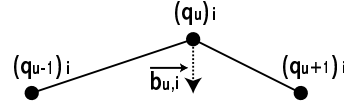the unity vector of q_u in radial direction in image i (See Figure 7).

Figure 7: Schematic representation of the unity vector $b_{u,i}$ of q_u in radial direction in image i.

The external force used to minimize the external energy of vertex q_u, i.e. $\overrightarrow{F_{ext}(q_u)}$, is a function of the external forces corresponding to the image planes:

$$
\begin{aligned}
\overrightarrow{F_{ext}(q_u)} &= f\left(\overrightarrow{F_{ext,1}((q_u)_1)}, \overrightarrow{F_{ext,2}((q_u)_2)}, \ldots, \right. \\
&\qquad \left. \overrightarrow{F_{ext,N}((q_u)_N)} \right) \qquad (10)
\end{aligned}
$$

The choice of the function f is important. Using three orthogonally recorded images,

$$\overrightarrow{F_{ext}(q_u)} = \frac{1}{2} \sum_{i=1}^{3} \overrightarrow{F_{ext,i}((q_u)_i)} \qquad (11)$$
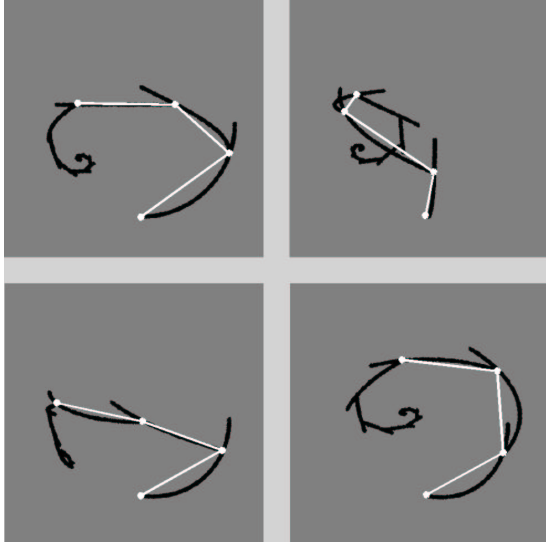
Figure 8: Four computer-generated phantom images with the indicated corresponding points (white markers), and the projections of the initial discrete dynamic curve (white lines).

can be used, but in general a linear combination is not suitable. We use:

$$
\begin{aligned}
\overrightarrow{F_{ext}(q_u)} = & \; \rho\Big((q_u)_1 + \overrightarrow{F_{ext,1}((q_u)_1)}, \\
& (q_u)_2 + \overrightarrow{F_{ext,2}((q_u)_2)}, \dots, \\
& (q_u)_N + \overrightarrow{F_{ext,N}((q_u)_N)}\Big) - q_u,
\end{aligned}
\tag{12}
$$

with ρ the reconstruction operator described in Section 2.2.

To conclude, deforming Q_u means replacing vertices q_u^{old} by:

$$
q_u^{new} = q_u^{old} + c_{if}\overrightarrow{F_{int}(q_u^{old})} + c_{ef}\overrightarrow{F_{ext}(q_u^{old})}.
\tag{13}
$$

By repeatedly resampling and deforming Q_u, the total energy $E_{total}(Q_u)$ and the error $\varepsilon(Q_u)$ minimize, or the discrete dynamic curve Q_u converges to the target curve T_v.

3 Results

The presented method is validated using computer-generated phantom images (See Figure 8). The ini-

tial discrete dynamic curve is obtained by indicating corresponding points in the images.

After 15 iterations, this means after 15 times resampling and deforming, a curve is obtained as presented in Figure 9 and Figure 10.
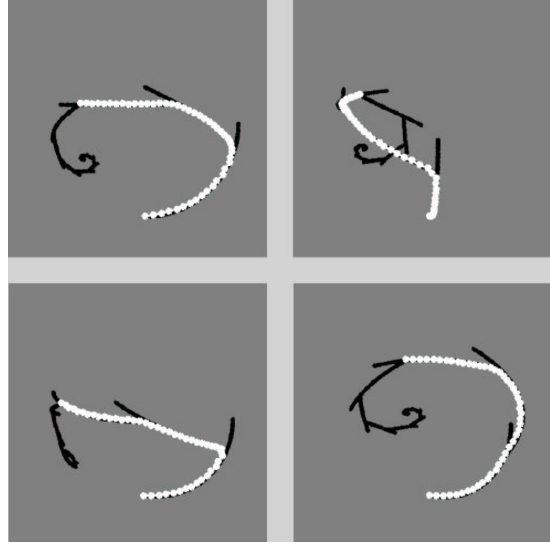

Figure 9: Four computer-generated phantom images with the projections of the discrete dynamic curve after 15 iterations.
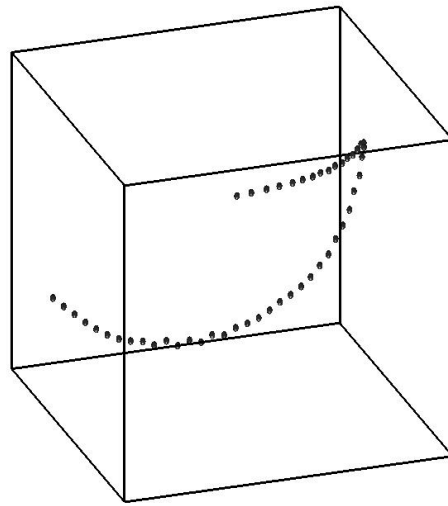

Figure 10: Three dimensional representation of the reconstructed centerline.

4 Conclusion

A method is presented to reconstruct the centerline of coronary arteries based on multiple (more than two) angiographic images using discrete dynamic curves. Using multiple images has the advantage that ambiguities about the centerline configuration become less likely. Extending the reconstructed centerline structure to a three dimensional reconstruction of the complete vessel structures will be the next step. Doing this using multiple images will theoretically result in a better reconstruction than using only two images.

References:

[1] J. Christiaens, R. Van de Walle, I. Lemahieu, P. Gheeraert and Y. Taeymans, Determination of QCA Parameters using Optimal Angiographic Viewing Angles, *Advances in Signal Processing and Computer Technologies*, WSES Press, 2001, pp. 133-138.

[2] T. Saito, M. Misaki, K. Shirato and T. Takishima, Three-Dimensional Quantitative Coronary Angiography, *IEEE Transactions on Biomedical Engineering*, 1990, vol. 37, pp. 768-77.

[3] D. Delaere, C. Smets, P. Suetens and G. Marchal; Knowledge-based system for the three-dimensional reconstruction of blood vessels from two angiographic projections, *Medical & Biological Engineering & Computing*, 1991, vol. 29, pp. NS27-NS36.

[4] C. Pellot et Al, A 3D Reconstruction of Vascular Structures from Two X-Ray Angiograms Using an Adapted Simulated Annealing Algorithm, *IEEE Transactions on Medical Imaging*, 1994, vol. 13, pp. 48-60.

[5] A. Wahle et Al, Assessment of Diffuse Coronary Artery Disiase by Quantitative Analysis of Coronary Morphology Based upon 3D Reconstructions from Biplane Angiograms, *IEEE Transactions on Medical Imaging*, 1995, vol. 14, pp. 230-41.

[6] R. Foroni et Al, Shape Recovery and Volume Calculation from Biplane Angiography in the Stereotactic Radiosurgical Treatment of Arteriovenous Malformations, *Int. J. Radiation Oncology Biol. Phys.*, 1996, vol. 35, pp. 565-77.

[7] S.Y. Chen & C.E. Metz, Improved determination of biplane imaging geometry form two projection images and its application to the three-dimensional reconstruction of coronary arterial trees, *Med Phys*, 1997, vol. 24, no. 5, pp. 633-54.

[8] P. Windyga et Al, Three-dimensional reconstruction of coronary arteries using a priori knowledge, *Medical & Biological Engineering & Computing*, 1998, vol. 36, pp. 158-64.

[9] S.J. Chen and J.D. Carroll, 3-D Reconstruction of Coronary Arterial Tree to Optimize Angiographic Visualization, *IEEE Transactions on Medical Imaging*, 2000, vol. 19, no. 4, pp. 318-336.

[10] A. Rougée, C. Picard, D. Saint-Fèlix, Y. Trousset, T. Moll and M. Amiel, Three-dimensional coronary arteriography, *International Journal of Cardiac Imaging*, 1994, vol. 10, pp. 67-70.

[11] C. Cañero, P. Radeva, R. Toledo, J.J. Villanueva and J. Mauri, 3D Curve Reconstruction by Biplane Snakes, *Proceedings of the 15th International Conference on Pattern Recognition (ICPR'00)*, 2000, vol. 4, pp. 563-566.

[12] A. Dumay, J. Reiber and J. Gerbrands, Determination of Optimal Angiographic Viewing Angles: Basic Principles and Evaluation Study, *IEEE Transactions on Medical Imaging*, 1994, vol. 13, no. 1, pp. 13-24.

[13] S. Lobregt and M. Viergever, A Discrete Dynamic Contour Model, *IEEE Transactions on Medical Imaging*, 1995, vol. 14, no. 1, pp. 12-24.